https://doi.org/10.46813/2022-140-025

SWELLING PREDICTION OF AISI 304 AND 18Cr10NiTi AUSTENITIC STAINLESS STEELS USING VARIOUS EMPIRICAL FUNCTIONS

A.S. Kalchenko, N.P. Lazarev
National Science Center "Kharkov Institute of Physics and Technology", Kharkiv, Ukraine
E-mail: kalchenko@kipt.kharkov.ua

A review of the known empirical dependences of austenitic steel swelling on in-reactor environments is carried out. The performance of empirical functions is compared in application to the conditions of thermal neutron reactor internals. Comparison with experimental data is made, and the influence of statistical errors of reactor data is discussed. Finally, the applicability of the empirical functions in the space of external parameters, precisely temperature, dose, and dose rate, is investigated.

PACS: 61.80.–x; 61.80.Az; 61.82.Bg

INTRODUCTION

Various empirical functions are widely used to describe temperature-dose dependences of swelling of austenitic steels [1–6]. Initially, these functions were developed for materials of fuel cladding and wrapper of fast reactors. However, there are currently attempts to use empirical functions to predict the swelling evolution in the thermal neutron reactor internals components. It is evident that the operating conditions of structural materials of fast reactor cores, such as EBR-II and BOR-60, are different from the operating conditions of the internals of thermal neutron reactors, which include PWRs and WWERs. The main difference is the dose rates, namely ~ 10^{-6} dpa/s for the fast and ~ 10^{-8} dpa/s for the thermal reactors. Modified functions are currently being developed to take this factor into account.

This paper discusses the empirical functions of swelling of the internals of thermal neutron reactors compared with those previously proposed for describing swelling in the core of fast reactor.

Creep-induced deformation must be considered when calculating the form change of PWR and WWER thermal neutron reactor internals components. The irradiation creep equation includes the swelling rate explicitly. Consequently, the irradiation component of creep will also depend on the behavior of the swelling rate. Therefore, we additionally consider the behavior of the swelling rate for conditions close to operating conditions in the internals of PWR and WWER reactors.

The basic materials of the internals are 18Cr10NiTi steel (chemically similar to AISI 321) in WWER reactors and AISI 304 steel (chemically similar to 18Cr9Ni) in PWR reactors. Therefore, these steels are chosen for comparison of the swelling description models.

EMPIRICAL FUNCTIONS OF SWELLING

One of the classical empirical functions most frequently mentioned in the literature is the Foster-Flinn equation, which was developed based on the swelling of AISI 304 steel irradiated in the core of the EBR-II fast reactor [1]. The Foster-Flinn equation describes swelling S as a function of temperature T and irradiation dose D, either as a power-low function of dose,

$$S_1(T,D)=\left(\frac{D}{5}\right)^2\cdot f(T), \tag{1}$$

$$f(T)=\exp\left\{-1.591+0.245\cdot T_0-1.210\cdot T_0^{\,2}-1.384\cdot T_0^{\,3}-1.204\cdot T_0^{\,4}\right\}, \tag{1a}$$

$$T_0=\frac{T-490}{100}, \tag{1b}$$

or has the form of a bilinear dose dependence,

$$S_2(T,D)=R_1(T)\cdot\frac{D}{5}+R_2(T)\cdot\left(\frac{D}{5}+\frac{1}{\alpha}\cdot\ln\left[\frac{1+\exp\{\alpha\cdot(\tau(T)-D/5)\}}{1+\exp\{\alpha\cdot\tau(T)\}}\right]\right), \tag{2}$$

$$R_1(T)=0.3481-0.3203\cdot T_1^2, \tag{2a}$$

$$R_2(T)=1.739+2.456\cdot T_1+2.505\cdot T_1^2-2.464\cdot T_1^3-5.222\cdot T_1^4, \tag{2b}$$

$$\tau(T)=3.674-0.231\cdot T_1+3.167\cdot T_1^2-0.695\cdot T_1^3-4.185\cdot T_1^4, \tag{2c}$$

$$T_1=\frac{T-460}{100},\ \alpha=0.8. \tag{2d}$$

Hereinafter, unless otherwise indicated, the following units are used: % – for swelling (S); ºC – for temperature (T); dpa – for irradiation dose (D); dpa/s – for dose rate (K).

Note that the original functions (1) and (2) in [1] have a dependence on the fluence measured in n/cm^2 units. In our paper, these functions are given as a function of irradiation dose in conventional dpa units, assuming that for a fast EBR-II reactor, we take the ratio 1 dpa = $2\cdot10^{21}$ n/cm^2 (E > 0.1 MeV) [7].

Based on the data at dose rates in the interval from $6\cdot10^{-9}$ to $3.6\cdot10^{-7}$ dpa/s presented in [8, 9], a modified Foster-Flinn equation was proposed, which is a function not only of temperature T and irradiation dose D, but also of the dose rate K [2]

$$S_3(T,D,K)=\left(\frac{D}{4.9}\right)^2\cdot g(K)\cdot f(T), \tag{3}$$

$$g(K)=\left(\frac{K}{1.25\cdot 10^{-7}}\right)^{-0.73}, \tag{3a}$$

where $f(T)$ is defined in Eq. (1a). The first two terms of Eq. (3) are written slightly differently in [3], and the temperature dependence was replaced by an Arrhenius-type function,

$$S_4(T,D,K)=D^2\cdot G(K)\cdot F(T), \tag{4}$$

$$G(K)=\left(\frac{K}{10^{-7}}\right)^{-0.731}, \tag{4a}$$

$$F(T)=\exp\left\{22.106-\left(\frac{18558}{T+273.15}\right)\right\}. \tag{4b}$$

To describe the swelling of 18Cr10NiTi steel, which is used as fuel cladding and wrapper of the BOR-60 fast reactor, a function of the following form was proposed in [4],

$$S_5(T,D)=R\cdot\left(D-D_0(T)\right)\cdot\exp\left\{-\beta\cdot\left(T-T_{\max}\right)^2\right\}, \tag{5}$$

where $D_0(T)=67-0.1T$ is the incubation dose dependent on irradiation temperature; $R=0.55$; $\beta=29\cdot 10^{-5}$; $T_{\max}=485$.

The function (5) was constructed for the dose rate interval from $0.4\cdot 10^{-6}$ to $1.4\cdot 10^{-6}$ dpa/s, which was not specified explicitly in [4]. It is stated in [4] that (5) makes it possible to evaluate changes in the material volume under inhomogeneous swelling of structural elements made of 18Cr10NiTi steel over the entire operating temperature range of the fast reactor BOR-60 core at damage doses up to ~ 100 dpa. This statement is based on the necessity of a linear approximation of swelling on dose in contrast to the often used power law since the linear dependence is predicted by the modern theory of irradiation effects in metals.

Nevertheless, the authors of [5] use the power law of the dose dependence of swelling. For this purpose, they summarized available proprietary and literature experimental data for dose rates in the interval from $1.3\cdot 10^{-7}$ to $8\cdot 10^{-7}$ dpa/s and proposed the following function to describe the swelling of steel AISI 304 [10],

$$S_6(T,D)=c\cdot D^{1.88}\cdot\exp\left\{-r\cdot\left(T-T_{\max}\right)^2\right\}, \tag{6}$$

where $c = 8.13\cdot 10^{-3}$; $r = 1.1\cdot 10^{-4}$; $T_{\max} = 470$.

It can be seen that functions (6) and (5) are composed in terms of dose and temperature only. Therefore, in order to predict the swelling at lower dose rates in the interval from $2\cdot 10^{-8}$ to $4.5\cdot 10^{-8}$ dpa/s by function (6), it is proposed [5] to multiply the coefficient c by 2 in Eq. (6).

To calculate the swelling of 18Cr10NiTi steel, the constants c and r should be changed to $c = 1.035\cdot 10^{-2}$, $r = 1.804\cdot 10^{-4}$ in Eq. (5) at dose rates in the interval from $3\cdot 10^{-7}$ to $6\cdot 10^{-7}$ dpa/s and changed to $c = 1.035\cdot 10^{-2}$, $r = 1.5\cdot 10^{-4}$ at dose rates in the interval from $0.6\cdot 10^{-8}$ to $8\cdot 10^{-8}$ dpa/s according to the paper [5]. It is proposed to use $c = 1.035\cdot 10^{-2}$, $r = 1.825\cdot 10^{-4}$ at dose rates both $(3…6)\cdot 10^{-7}$ dpa/s, and $(0.7…8)\cdot 10^{-8}$ dpa/s according to the paper [10].

Taking function (5) as the basis and using experimental data on swelling obtained in the fast reactor and under ion irradiation, an empirical swelling function for 18Cr10NiTi steel was developed in [6] that depends not only on temperature and dose but also on the dose rate in a wide range from 10^{-2} to 10^{-6} dpa/s. Subsequently, this function has been extrapolated to lower dose rates up to 10^{-8} dpa/s, typical for pressure vessel internals of thermal reactors [11],

$$S_7(T,D,K)=R(K)\cdot\phi\left(D-D_0(T,K)\right)\cdot\exp\left\{-\frac{\left(T-T_{\max}(K)\right)^2}{2\cdot\sigma_T^2(K)}\right\}, \tag{7}$$

where $\varphi(x)=x\cdot\theta(x)$ and $\theta(x)$ is the Heaviside unit step function: $\theta(x)=1,\ x>0$ or $0,\ x\le 0$; $R(K)=r_0-r_k\ln K$ is the swelling rate at the steady state; $D_0(T,K)=d_0-d_T T+d_k\ln K$ is the incubation period; $T_{\max}(K)=T_0+T_k\ln K$ is the peak swelling temperature; $\sigma_T(K)=\sigma_0-\sigma_k\ln K$ is the temperature dispersion. r_0 = 0.25; r_k = 0.022; d_0 = 103; d_T = 0.1; d_k = 2.6; T_0 = 690; T_k = 15.5; σ_0 = 12.3; σ_k = 1.9.

Note that function (7) is a function (5) modification, in which the constants R, β, $T_{\max}$ are replaced by parametric functions of the dose rate K. The temperature-dependent incubation period $D_0(T)$ in Eq. (5) also became dependent on the dose rate $D_0(T,K)$ in Eq. (7). Thus, the function (7) directly depends on the dpa rate, and there is no need to adjust the constants when passing from one irradiation condition to another.

DISCUSSION

Experimental data [1] on dose dependences of swelling of AISI 304 steel irradiated in the EBR-II reactor in the temperature range of 400…500 °C are shown in Fig. 1,a, on which the empirical swelling functions (1) and (2) at 450 °C are plotted (solid lines).

At low doses (< 30 dpa), both the power function (1) and the bilinear function (2) describe the experimental data approximately equally. However, at doses > 30 dpa, these empirical functions give significantly different predictions. For example, while function (1) predicts a swelling of 64 % at 100 dpa, function (2) predicts the swelling of two times less of 31 % at the same irradiation dose. This behavior is easily explained if we consider the swelling rates shown as dashed lines in Fig. 1,a. It can be seen that the swelling rate of function (1) increases linearly with irradiation dose and is 0.59 %/dpa at 46 dpa for the experimental point with maximum reduced swelling. On the other hand, the swelling rate of function (2) increases monotonically in the dose interval of 0…30 dpa at approximately the same rate as the swelling rate of function (1), after which it reaches saturation of 0.37 %/dpa. Therefore, coming to a constant of swelling rate $dS_2/dD=\text{const}$ indicates that function (2) has reached a steady-state swelling stage. Accordingly, the previous stage in the dose interval 0…30 dpa, where $dS_2/dD\ne\text{const}$ indicates the transient swelling stage of the function (2).

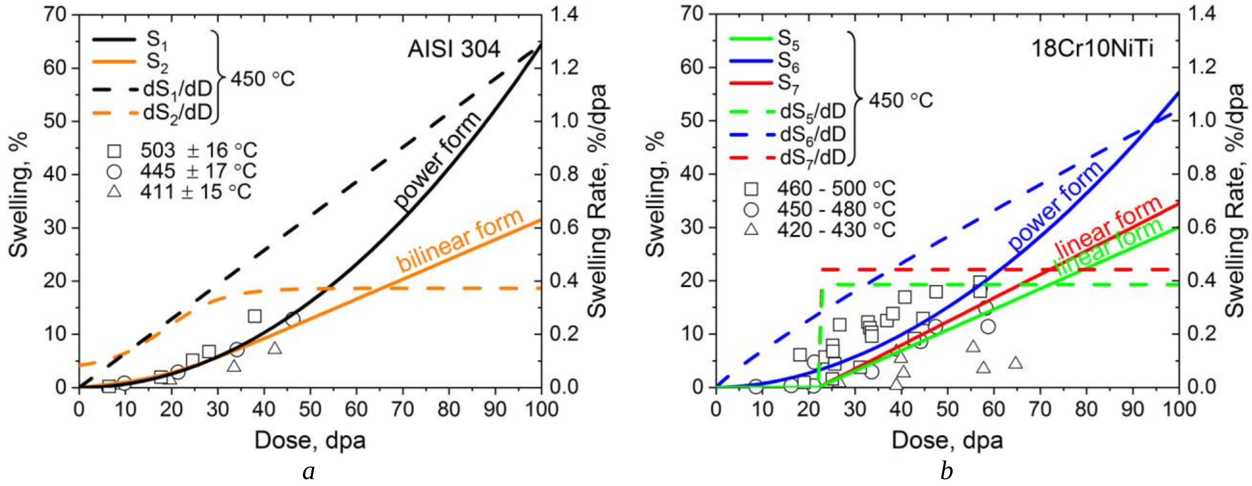

Fig. 1. Dose dependences of swelling (solid lines) and swelling rate (dashed lines) of (a) AISI 304 steel and (b) 18Cr10NiTi steel at dose rates typical of fast reactors ($K = 10^{-6}$ dpa/s). The symbols show the experimental data from [1] and [4], for (a) and (b), respectively

Consequently, returning to the function (1), we can state that this function S_1 does not assume a steady-state swelling stage over the entire irradiation dose interval since its derivation dS_1/dD will never be a constant. Thus, function (1) always describes swelling only in the transient stage at any irradiation dose.

Fig. 1,b shows experimental data [4] on the dose dependences of the swelling of 18Cr10NiTi steel irradiated in the BOR-60 reactor in the temperature range 420…500 °C together with the empirical swelling functions (5), (6), and (7) at 450 °C (solid lines). Recall that the authors of [4] stated that function (5) allows evaluating the swelling of 18Cr10NiTi steel over the operating temperature range of BOR-60 fast reactor core at damage doses up to ~ 100 dpa. In this case, function (5) predicts 30 % at 450 °C. Function (7) predicts a relative swelling value of 34 %. Function (6) predicts a swelling of 55 %, which is almost twice as high as expected by function (5).

Thus, it can be concluded that at 450 °C and an irradiation dose of 100 dpa, the power functions (1) and (6) predict swelling about twice as much as the bilinear function (2) and linear functions (5) and (7).

Functions (5) and (7) are of the threshold nature of the dose dependence of swelling with a subsequent increase in swelling linearly proportional to the damage dose. This transition is clearly recorded by the derivatives of swelling on the irradiation dose in the form of swelling rate steps (green and red dotted lines in Fig. 1,b). The absolute value of the steps are $dS_5/dD = 0.38\,\%/\,\mathrm{dpa}$ and $dS_7/dD = 0.44\,\%/\,\mathrm{dpa}$. These values are the swelling rates at the steady-state stage at a given irradiation temperature of 450 °C. Thus, these functions describe the dose dependence of swelling in the form of a certain incubation period with a sharp transition to the stationary stage of swelling.

Function (6) has a power-law dependence on the irradiation dose. In contrast to the previously considered function (1), where the exponent of the damage dose was 2, function (6) has an exponent of 1.88. This feature shows that the swelling rate of function (6) is not linear but proportional to $D^{0.88}$. Similar to function (1), the function (6) does not provide for a steady-state swelling stage in the dose interval up to 100 dpa, since dS_6/dD never becomes a constant.

Experimental data on swelling of AISI 304 steel irradiated in EBR-II reactor [1] and 18Cr10NiTi steel irradiated in the BOR-60 reactor [4] at irradiation doses of 40…50 dpa in a wide temperature range are presented in Fig. 2,a. The temperature dependences of swelling of AISI 304 and 18Cr10NiTi steels calculated by various empirical functions at an average dose for the experimental data of 45 dpa are also plotted there.

The temperature dependences of the functions shown in Fig. 2,a have a familiar bell-shaped appearance. As the irradiation temperature increases, the swelling increases to some peak value, and then the swelling decreases. Functions (5), (6), and (7) describe the temperature dependence using a Gaussian function. Functions (1) and (2) describe this dependence as an exponent of the polynomial of the fourth power. Functions (1) and (2) have no symmetry relative to the temperature maximum, and their maxima are shifted towards higher irradiation temperatures. The experimental data presented here show that AISI 304 steel swells higher than 18Cr10NiTi at temperatures below the swelling maximum (400…450 °C). This trend is demonstrated by functions (1), (2), (5), and (7), which cannot be said about function (6). This function demonstrates that swelling inversion occurs in a given temperature range. Function (6) shows that AISI 304 swells stronger than 18Cr10NiTi at 400…415 °C and weaker at 415…450 °C. The temperature peak of swelling of AISI 304 steel reaches 17 % at 500 °C according to (1), 17 % at 510 °C for (2), and 10 % at 470 °C for function (6). The temperature peak of swelling of 18Cr10NiTi steel has closer values for both temperature and swelling: 15 % at 490 °C (5), 13 % at 470 °C (6), and 14 % at 480 °C (7). Function (6) predicts a wider swelling temperature interval than (5) and (7).

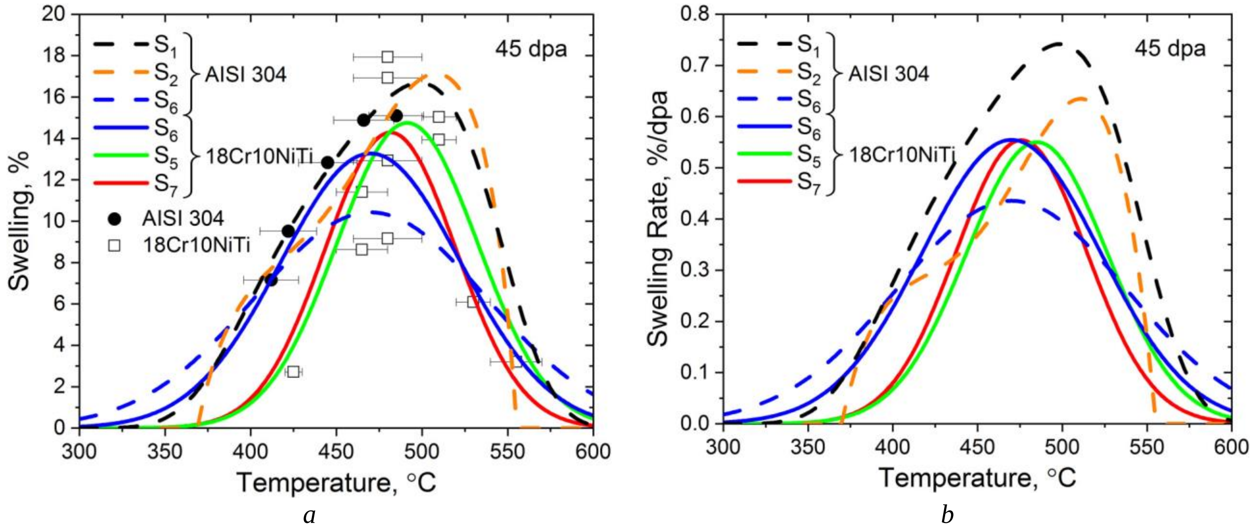

Fig. 2. Temperature dependences of (a) swelling and (b) swelling rates of AISI 304 steel (dashed lines) and 18Cr10NiTi steel (solid lines) at dose rates typical of fast reactors ($K = 10^{-6}$ dpa/s) calculated at 45 dpa. The symbols in (a) show experimental data for AISI 304 steel (shaded/darkened) at D = 42…46 dpa from [1] and for 18Cr10NiTi steel (unshaded/lightened) at D = 40…50 dpa from [4]

Temperature dependences of swelling rate in Fig. 2,b are similar to the corresponding swelling dependences in Fig. 2,a at a dose of 45 dpa. However, the maximum swelling rate of AISI 304 steel appears to be different for the empirical functions considered: 0.74 %/dpa at 500 °C (1), 0.63 %/dpa at 510 °C (2), and 0.43 %/dpa at 470 °C (6). At the same time, for 18Cr10NiTi steel, the maximum swelling rate is 0.55 %/dpa and lies in the temperature range 470…490 °C, according to functions (5), (6), and (7).

Recall that functions (3) and (4) are modifications of function (1), since the latter was developed only for the EBR-II reactor. The same applies to function (5), which can only be used to calculate structural elements of the BOR-60 reactor core made of 18Cr10NiTi steel. In the case of function (6), according to [5], it is necessary to change the values of the corresponding parameters to switch from the irradiation conditions of a fast reactor to the conditions in a thermal neutron reactor. However, it is stated in [10] that this is unnecessary for 18Cr10NiTi steel. For function (7), nothing needs to be changed, and you need to insert the variables of interest, irradiation temperature, dose, and dose rate [6, 11].

Fig. 3,a presents the temperature dependences of swelling calculated using functions (3), (4), (6), and (7) at a dose of 45 dpa. Fig. 3,b presents the temperature dependences of the swelling rate (obtained by differentiating these functions by the damage dose) for the dose rates typical of the thermal neutron reactor internals components.

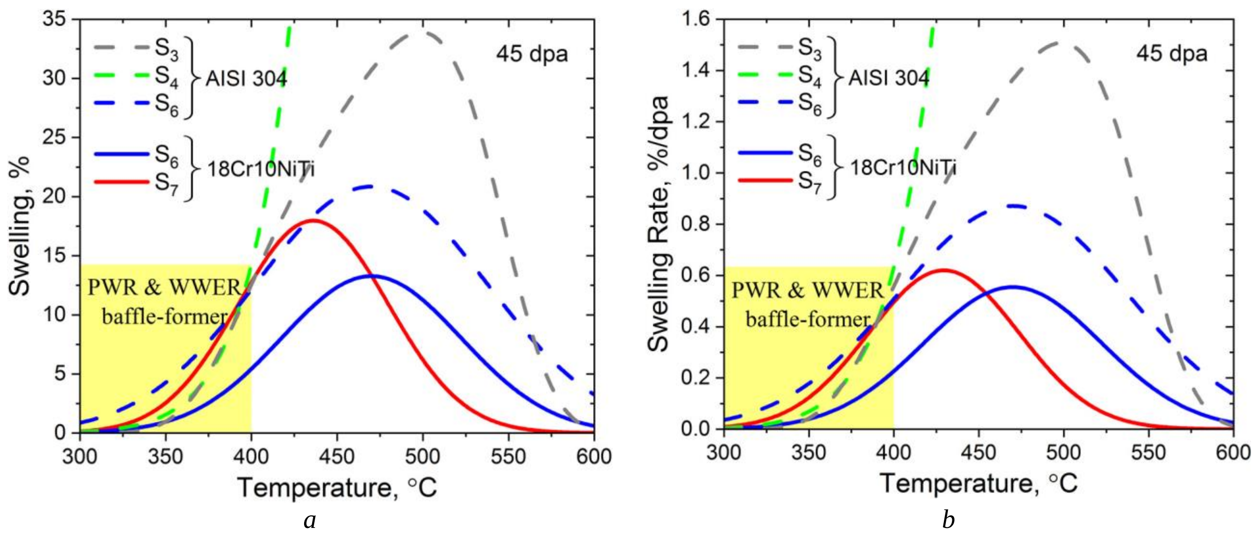

Fig. 3. Temperature dependences of (a) swelling and (b) swelling rates of AISI 304 steel (dashed lines) and 18Cr10NiTi steel (solid lines) at dose rates typical for thermal reactors ($K = 5 \cdot 10^{-8}$ dpa/s) calculated at 45 dpa. The yellow color highlights the area of temperatures typical for operation of the baffle-formers, the pressure vessel internals of PWRs and WWERs

The appearance of the temperature dependences of the swelling and swelling rate functions (3) and (4) is different, even though they were obtained based on the same set of experimental data on the swelling of AISI 304 steel [8, 9] (compare the dashed gray and green lines in Fig. 3,a and b, respectively). The swelling and swelling rate of function (3) has a bell-shaped appearance similar to that discussed above for function (1). Function (4) increases rapidly with increasing irradiation temperature and does not have a temperature maximum of either the swelling or the swelling rate. Both function (3) and function (4) behave approximately equally at temperatures of 300…390 °C, but at higher temperatures, the swelling and swelling rate of function (4) are much higher. At their intersection point of 390 °C, these functions exhibit a swelling rate of 0.42 %/dpa. The swelling and swelling rate function (6) calculated for AISI 304 steel (dashed blue lines in Fig. 3) intersect the functions (3) and (4) at a temperature of about 390 °C. Both swelling and swelling rate of function (6) are higher than those of (3) and (4) at T < 390 °C, while at the higher temperature, it is lower.

The temperature dependences of swelling and swelling rate of 18Cr10NiTi steel calculated using functions (6) (solid blue lines in Fig. 3) have maximums of 13 % and 0.55 %/dpa at 470 °C. For function (7) (solid red lines in Fig. 3), the same maximums are 18 % and 0.62 %/dpa at 430 °C. Function (7) predicts a higher swelling value than function (6) at T < 470 °C, and vice versa, a lower one at T > 470 °C. The same trend holds for the swelling rate, but the temperature at which this transition occurs is 455 °C.

It should be noted the ambiguity in the behavior of temperature dependences of swelling of steels AISI 304 and 18Cr10NiTi calculated by function (6) at different dose rates. For example, if the temperature maximum of swelling is higher in 18Cr10NiTi steel at dose rate typical for fast reactors ($K = 10^{-6}$ dpa/s) (see Fig. 2), on the contrary, the steel AISI 304 swells stronger within the whole range of temperatures at dose rate typical for thermal reactors ($K = 5{\cdot}10^{-8}$ dpa/s) (see Fig. 3).

Swelling is affected by various operational factors, such as irradiation temperature, damage dose, dose rate, simultaneous introduction of helium and hydrogen, etc., which are difficult to determine accurately under reactor conditions. As a rule, the statistical errors of reactor data are substantial since the history of thermal and neutron fields for a particular sample is not accurately traced. Therefore, calculated data are used for these quantities, which are not always accurate. For example, an error of 10…20 °C in determining the irradiation temperature leads to a relatively significant shift in the average swelling value. Fig. 2,a shows that the statistical scatter of swelling can reach 10…30 % in this case. Thus, empirical dependences for the calculation of swelling should be considered only with an indication of the interval of the main parameters and the confidence band of function values.

The dependence of swelling on the dose is always nonlinear. It is evident in the incubation and transient stages of swelling. For the late stage, a simple rate theory predicts some slow decrease in the swelling rate with dose, see Appendix for details. However, we do not consider this weak nonlinearity because it is incomparably smaller than the confidence interval of the experimental data. Therefore, the linear dependence of swelling on dose seems to be the most reasonable and adequate to the known experimental data at a later stage.

As follows from the rate theory, at the beginning of the transient stage, we can expect a dependence of the form $S \sim \left(D - D_0\right)^{\alpha}$, where α = 3/2. Some empirical functions (1), (3), (4), and (6) use a more prominent exponent, α = 2 and α = 1.88, in order to capture also some part of the incubation stage. Obviously, for large doses, such parameterization is entirely inappropriate. The applicability of such power-dose functions is limited only to the transient stage.

The swelling rate cannot increase indefinitely, and it reaches a steady state upon completion of the transient processes. For example, the duration of transient processes of the dislocation structure usually does not exceed about 30 dpa, both for annealed and cold-worked austenitic steels [13–15]. The end of transient swelling processes and reaching the steady state about 30 dpa are demonstrated only by bilinear (2) and linear (5), (7) empirical functions. Thus, the 45 dpa in Figs. 2 and 3 is the dose of the steady-state swelling stage, above which the swelling rate should not increase. Therefore, the calculation of swelling using functions (1), (3), (4), and (6) at doses greater than 45 dpa is inappropriate.

It is well known that the baffle-former of PWR and WWER reactors has the most stressful operating conditions among all pressure vessel internals. Locally, the operating temperature of the baffle-former of a thermal reactor can reach 370…400 °C due to gamma heating. It is suggested in [12] that for pressure vessel internals of thermal reactors, a swelling rate of about 0.07 %/dpa should be expected at low temperatures (< 370 °C) and low operating doses. In our case, a calculation using various empirical functions gives a swelling rate of 0.09 to 0.29 %/dpa at T = 370 °C and D = 45 dpa (see Fig. 3,b). However, as can be seen from Fig. 3b, the predicted swelling rate is very sensitive to the irradiation temperature. If the maximum of swelling rate does not exceed 0.04 %/dpa at T = 300 °C, it can reach 0.22…0.63 %/dpa at T = 400 °C, depending on the chosen empirical function.

CONCLUSIONS

At low irradiation doses, the power function (1) and the bilinear function (2) appear similar, but for higher doses, they diverge significantly. The power function (1) is adjusted to fit the experimental data of the transient stage and appears irrelevant for high irradiation doses. At high doses, function (2) seems more appropriate.

Dose dependence of swelling (5) describes swelling of 18Cr10NiTi steel in the form of a linear function with some incubation period. Such linear dependence at high damage doses is justified and satisfactorily describes data for a fast reactor. This parameterization, though, appears inapplicable in conditions specific to the internals of WWER.

Functions (1), (2), and (5) are the functions of just two variables, precisely dose, and temperature, and can be applied exclusively for steels used as core structural components of fast reactors.

Functions (3) and (4) are designed exclusively for low dose rates of (0.06…3.60)·10^{-7} dpa/s and are the functions of the dose, temperature and dose rate, but are valid only at a transient swelling stage and have been tested only for AISI 304 steels.

Function (6) is the function of only dose and temperature. Ignoring the dose rate makes the function too average for describing the swelling of the reactor's structural components. It gives a satisfactory description of the dose swelling dependence only at the transient stage. The function cannot be applied to predict high irradiation dose swelling.

Function (7) is developed based on the ion irradiation data and the fast reactor data at dose rates in the interval from 10^{-2} to 10^{-6} dpa/s. It gives swelling dependence in a wide range of doses, temperatures, and dose rates, describing the averaged swelling fields and locating dangerous irradiation damage sites. Therefore, this function seems the most relevant for predicting WWER reactor internals swelling.

APPENDIX

Theoretical background of phenomenological description

Under irradiation, a knock-on atom displaces from its lattice site. As a result, a vacant site appears, and the knocked-out atom forms an interstitial type defect. The number of vacant sites coincides with the number of self-interstitial atoms (SIA). Due to diffusion, point defects can approach. While defects of different signs annihilate, defects of the same signs combine into complexes. The merger of SIAs forms dislocation loops. In turn, vacancy complexes can exist as vacancy dislocation loops and voids. If only dislocation loops arise, then the change in volume associated with interstitial loops is compensated by the change in volume associated with vacancy loops. If there are voids, there is a positive volume change. The voids are responsible for the overall volume change since it is equal to the volume of dislocation loops that have climbed to the external surface.

The conventional theory of irradiation damage is formulated using the mean-field chemical rate equations [16–18]. It describes microstructure evolution, including voids, gas bubbles, dislocation loops, new phase precipitates, grain boundaries, etc. The cornerstone of the theory is the concept of bias, which provides the separation of vacancy and SIA fluxes into different microstructure subsystems. This concept was first proposed to describe the preferential trapping of SIAs at dislocations, leading to an excess of vacancies, which provides the void/bubble growth [19]. Subsequently, this idea was supplemented by the possibility of forming overbalanced vacancies under cascade damage conditions [20]. An overview of the current state of irradiation rate theory can be found elsewhere [21].

As an illustration, let us consider a simple swelling model at fixed densities of extended defects, namely dislocations, voids, and other neutral sinks, including grain boundaries, incoherent precipitates etc. In this case, the average point defect concentrations are determined by [16],

$$K_p - \alpha C_i C_v - k_p^2 D_p C_p = 0,\qquad \text{(A.1)}$$
$$k_p^2 = Z_p \rho + n + 4\pi R b,$$

where index $p = i, v$ is attributed to SIAs and vacancies, respectively; C_p and D_p are the concentration and diffusivity of p-defect; $\alpha = 4\pi r_{iv}(D_i + D_v)$ is the recombination coefficient; r_{iv} is the radius of vacancy-SIA recombination; ρ is the dislocation density with fixed bias factor Z_i for SIAs and Z_v for vacancies; n is the strength of neutral sinks; $4\pi Rb$ is the sink strength of voids of density b and average radius R. The generation rate of point defects K_p also incorporates thermal emission of p-defects from extended defect: $K_p = K_p^0 + K_p^{\text{th}}$. Thermal emission of vacancies has the form

$$K_v^{\text{th}} = (Z_v \rho + n) D_v C_v^0 + 4\pi R b D_v C_v^b,\qquad \text{(A.2)}$$
$$C_v^0 = \exp(-E_v^f / T),$$
$$C_v^b = C_v^0 \exp(2\sigma v_a / RT),$$

where E_v^f is the vacancy formation energy; T is the temperature; v_a is the atomic volume; σ is the surface energy. Traditionally, thermal evaporation of SIAs is neglected, $K_i^{\text{th}} = 0$.

Swelling is defined by total volume of voids: $S = 4\pi \langle r^3 \rangle b / 3$, where $\langle r^3 \rangle$ is the average cube of the void radius. The growth rate of void of radius r is defined by vacancy and SIA fluxes, $dV/dt = 4\pi r \left(D_v C_v - D_v C_v^b - D_i C_i \right)$. Further, for the sake of simplicity, we assume that $\langle r^3 \rangle = R^3$. Within the framework of the made approximations the swelling rate reads [16]

$$\frac{dS}{dD} = \frac{(Z_i - Z_v) 4\pi R b \rho}{(Z_v \rho + n + 4\pi R b)^2} F(\eta),\qquad \text{(A.3)}$$

where $D = Kt$ is the irradiation dose; t is the time; $F(\eta)$ is the function of the temperature dependent parameter $\eta = 4\alpha K / D_i D_v k_i^2 k_v^2$. The analytical form of function $F(\eta)$ is rather cumbersome [16]. For our purposes, it is sufficient to know that the function $F(\eta)$ tends to zero both at low temperature, when recombination dominates, and at high temperature, when thermal emission of vacancies prevents void growth. At intermediate temperature this function has maximum and $F(\eta) \cong 1$.

Obviously, the correct description of swelling as a function of time should include time-dependent densities of dislocations and voids. It was observed that regardless of the initial dislocation density, it evolves rapidly to the saturation value that depends on temperature and dose rate but has little dependence on the magnitude of the dose [13]. The steady-state dislocation density at the temperature maximum region is about $\rho \sim 10^{10}$ cm^{-2} in austenitic stainless steel.

By considering the realistic size distribution of voids, it was shown that at the initial stage of swelling the void nucleation rate has a significant effect on the density of voids. With time, due to the thermal coarsening of the void ensemble, the density of voids comes out to some weakly time-dependent value. At high temperature in the void-dominated regime, the time dependence of the void density is asymptotically proportional to $b(t) \sim t^{-1/6}$ [22, 23]. The void density's time dependence seems even weaker in the region of the peak swelling temperature.

Assuming fixed dislocation and void densities, as well as in temperature region where $F(\eta) = 1$, we solve equation (A.3). The solutions are shown in Fig. A.1 for three different void densities.

Let us consider asymptotic solutions of equation (A.1) to interpret the dependencies shown in Fig. A.1. At small dose, when $4\pi Rb \ll Z_v\rho + n$, the swelling rate increases with dose as $dS/dD \sim \sqrt{D - D_0}$ and the swelling scales as $S \sim (D - D_0)^{3/2}$. At high dose, when void sink dominates, $4\pi Rb >> Z_v\rho + n$, the swelling rate drops with dose as $dS/dD \sim (D - D_0)^{-1/4}$, and the swelling dose dependence becomes $S \sim (D - D_0)^{3/4}$.

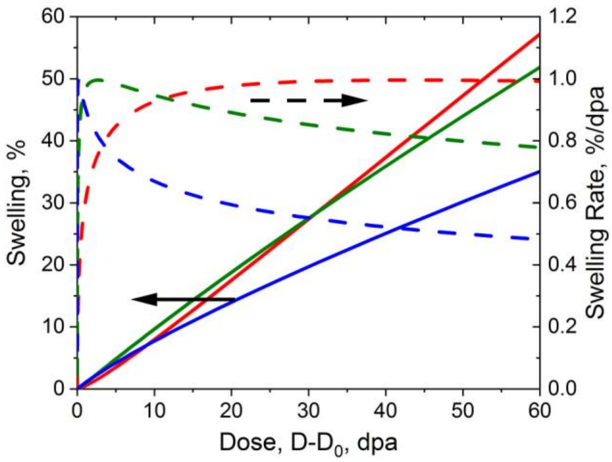

Fig. A.1. Dependence of swelling (solid lines) and swelling rate (dashed lines) on the dose at different void densities: 0.25·10^{16} cm^{-3} – red lines, 1·10^{16} cm^{-3} – green lines, 4·10^{16} cm^{-3} – blue lines. Parameters: temperature is T = 480 °C, dose rate is 10^{-6} dpa/s; cascade efficiency is 0.4, dislocation density is $\rho = 5\cdot 10^{10}$ cm^{-2}; density of neutral sinks is $n = \rho$; bias factor is $Z_i - Z_v = 0.2$. Material parameters for austenitic stainless steel were taken from [13]. The dose is shifted by the amount of the incubation dose D_0, which must be determined independently

Obviously, in the intermediate time domain, the swelling rate reaches a maximum and then slowly decreases. The dose to get the maximum swelling rate decreases with increasing void density b.

An important observation from Fig. A.1 is that the steady-state swelling rate slowly decreases by no more than a factor of 2 when the shifted dose $D - D_0$ changes by more than two orders of magnitude. A more realistic model [23] that self-consistently determines the change in void density with dose show an even slighter decrease in the swelling rate $dS/dD \sim (D - D_0)^{-1/6}$.

ACKNOWLEDGEMENTS

Authors would like to thank Frank Garner for fruitful discussions.

This work was financially supported by the National Academy of Science of Ukraine (program "Fundamental scientific research on the most important problems of the development of scientific and technical, socio-economic, socio-political, human potential to ensure Ukraine's competitiveness in the world and sustainable development of society and the state").

REFERENCES

1. J.P. Foster, J.E. Flinn. Residual stress behavior in fast neutron irradiated SA AISI 304 stainless steel cylindrical tubing // *J. Nucl. Mater*. 1980, v. 89, p. 99-112; https://doi.org/10.1016/0022-3115(80)90014-8
2. T. Tanaka, et al. Measurement of Damage Rate Dependence on Swelling of 304SA Stainless Steel // *Fall meeting of the Atomic Energy Society of Japan*, 2002, p.705.
3. F.A. Garner. Void swelling and irradiation creep in light water reactor environments // *Philip G. Tipping, Understanding and Mitigating Ageing in Nuclear Power Plants: Materials and Operational Aspects of Plant Life Management (PLiM)*. Woodhead Publishing, Philadelphia, PA, 2010, p. 914 (Chapter 10); https://app.knovel.com/kn/resources/kpUMANPPM2/toc
4. S.N. Votinov, V.I. Prokhorov, and Z.E. Ostrovsky. *Irradiated stainless steels*. Nauka publ., 1987, p.128.
5. N.K. Vasina, B.Z. Margolin, A.G. Gulenko, I.P. Kursevitch. Radiation swelling of austenitic steels: the influence of various factors: Experimental data processing and formulation of governing equations // *Problems of Materials Science*. 2006, N 4(48) p. 69-89.
6. A.S. Kalchenko, V.V. Bryk, N.P. Lazarev, I.M. Neklyudov, V.N. Voyevodin, F.A. Garner. Prediction of swelling of 18Cr10NiTi austenitic steel over a wide range of displacement rates // *J. Nucl. Mater*. 2010, v. 399, p. 114-121; https://doi.org/10.1016/j.jnucmat.2010.01.010
7. F.A. Garner. *Radiation-Induced Damage in Austenitic Structural Steels Used in Nuclear Reactors* / Konings, Rudy J.M. and Stoller Roger E. (eds.) Comprehensive Nuclear Materials 2nd edition, 2020, v. 3, p. 57-168. Oxford: Elsevier; http://dx.doi.org/10.1016/B978-0-12-803581-8.12067-3
8. G.M. Bond, B.H. Sencer, F.A. Garner, M.L. Hamilton, T.R. Allen, and D.L. Porter. Void Swelling of Annealed 304 Stainless Steel at ~ 370–385 °C and PWR-relevant Displacement Rates' // *9th International Conference on Environmental*

Degradation of Materials in Nuclear Power Systems – Water Reactors, 1999, p. 1045-1050; https://doi.org/10.1002/9781118787618.ch109

9. F.A. Garner, D.J. Edwards, S.M. Bruemmer, S.I. Porollo, Yu.V. Konobeev, V.S. Neustroev V.K. Shamardin, and A.V. Kozlov. Recent Developments Concerning Potential Void Swelling of PWR Internals Constructed from Austenitic Stainless Steels // *Proc. Fontevraud 5, Contribution of Materials Investigation to the Resolution of Problems Encountered in Pressurized Water Reactors,* September 23–27, 2002, on CD format, no page numbers.

10. I.P. Kursevich, G.P. Karzov, B.Z. Margolin, A.A. Sorokin, I.V. Teplukhina, Principles of alloying a novel radiation-resistant austenitic steel for the VVER-1200 reactor internals guaranteeing their safe operation for at least 60 years // *Inorganic materials: applied research*. 2013, N 4, p. 575-584; https://doi.org/10.1134/S2075113313060099

11. A.S. Kalchenko, V.V. Bryk, N.P. Lazarev, V.N. Voyevodin, and F.A. Garner. Prediction of void swelling in the baffle ring of WWER-1000 reactors for service life of 30-60 years // *J. Nucl. Mater*. 2013, v. 437, p. 415-423; https://doi.org/10.1016/j.jnucmat.2013.02.010

12. F.A. Garner. New data and insights on prediction of void swelling in austenitic pressure vessel internals // *Proceedings Fontevraud 9 – Contribution of Materials Investigations and Operating Experience to Light Water NPPs' Safety, Performance and Reliability*, 2018.

13. W.G. Wolfer, B.B. Glasgow. Dislocation evolution in metals during irradiation // *Acta Metallurgica.* 1985, v. 33, p. 1997-2004; https://doi.org/10.1016/0001-6160(85)90122-1

14. F.A. Garner, W.G. Wolfer. Effects of Radiation on Materials // *11th Conference, ASTM STP 782.* Brager H.R., Perrin J.S. (eds). American Society for Testing and Materials, West Conshohocken, PA, 1982, p 1073.

15. F.A. Garner. *Materials Science and Technology*. Frost BRT (ed), chap 6, v. 10A. VCH, New York, 1994, p. 419.

16. A.D. Brailsford, R. Bullough, The rate theory of swelling due to void growth in irradiated metals // *Journal of Nuclear Materials.* 1972, v. 44, p. 121-135; https://doi.org/10.1016/0022-3115(72)90091-8

17. H. Wiedersich. On the theory of void formation during irradiation // *Radiation Effects.* 1972, v. 12, p. 111-125; https://doi.org/10.1080/00337577208231128

18. J.L. Katz, H. Wiedersich. Nucleation of voids in materials supersaturated with vacancies and interstitials // *The Journal of Chemical Physics*. 1971, v. 55, p. 1414; https://doi.org/10.1063/1.1676236

19. G.W. Greenwood, A.J.E. Foreman, D.E. Rimmer. The role of vacancies and dislocations in the nucleation and growth of gas bubbles in irradiated fissile material // *Journal of Nuclear Materials.* 1959, v. 1, p. 305-324; https://doi.org/10.1016/0022-3115(59)90030-3

20. C.H. Woo, B.N. Singh. The concept of production bias and its possible role in defect accumulation under cascade damage conditions // *Physica Status Solidi (b).* 1990, v. 159, p. 609-616; https://doi.org/10.1002/pssb.2221590210

21. S.I. Golubov, A.V. Barashev, R.E. Stoller. Reaction Rate Theory // *Comprehensive Nuclear Materials.* R.J.M. Konings, R.E. Stoller (eds), (2nd Edition). Elsevier, 2020, p. 717-753; https://doi.org/10.1016/B978-0-12-803581-8.00663-9

22. L.A. Maksimov, A.I. Ryazanov. Kinetics of void coalescence in a crystal with dislocations under conditions of volumetric generation of point defects // *Radiation Effects.* 1977, v. 3, p. 1-5; https://doi.org/10.1080/00337577708233082

23. V.I. Dubinko, P.N. Ostapchuk, V.V. Slezov. Theory of radiation-induced and thermal coarsening of the void ensemble in metals under irradiation // *Journal of Nuclear Materials*. 1989, v. 161, p. 239-260; https://doi.org/10.1016/0022-3115(89)90488-1

Article received 06.06.2022

ПРОГНОЗУВАННЯ РОЗПУХАННЯ АУСТЕНІТНИХ НЕРЖАВІЮЧИХ СТАЛЕЙ AISI 304 І Х18Н10Т ЗА ДОПОМОГОЮ РІЗНИХ ЕМПІРИЧНИХ ФУНКЦІЙ

О.С. Кальченко, М.П. Лазарев

Проведено огляд відомих емпіричних залежностей розпухання аустенітної сталі при реакторному опроміненні. Порівнюється ефективність емпіричних функцій щодо умов внутрішньо-корпусних пристроїв реактора на теплових нейтронах. Проведено порівняння з експериментальними даними, обговорюється вплив статистичних помилок реакторних даних. Нарешті, досліджується застосовність емпіричних функцій в залежності від зовнішніх параметрів, а саме температури, дози та швидкості створення зсувів.